Upscaling fixed bed adsorption behaviors towards emerging micropollutants in treated natural waters with aging activated carbon Model development and validation

Ni Ye, Nicolas Cimetiere, Véronique Heim, Nils Fauchon, Cédric Feliers, Dominique Wolbert

1 **Upscaling fixed bed adsorption behaviors towards emerging**

2 **micropollutants in treated natural waters with aging activated**

3 **carbon: model development and validation**

4

5 Ni YE[*,a,b], Nicolas CIMETIERE[a], Véronique HEIM[c], Nils FAUCHON[b], Cédric FELIERS[b],

6 Dominique WOLBERT[a]

7 (a) Univ. Rennes, Ecole Nationale Supérieure de Chimie de Rennes, CNRS, ISCR - UMR

8 6226, F - 35000 Rennes, France

9 (b) Veolia Eau d'Ile de France, 28 boulevard Pesaro, TSA 31197, 92739 Nanterre, France

10 (c) Syndicat des Eaux d'Ile de France, 120 boulevard Saint Germain, 75006 Paris

11 E-mail address: ni.ye@veolia.com

12 nicolas.cimetiere@ensc-rennes.fr

13 v.heim@sedif.com

14 nils.fauchon@veolia.com

15 cedric.feliers@veolia.com

16 dominique.wolbert@ensc-rennes.fr

17 *   Corresponding author:

18 E-mail address: ni.ye@veolia.com

19

20

1

Abstract

A scale-up procedure was assessed in this study to predict the fixed bed adsorption behaviors with aging granular activated carbon (GAC) for various micropollutants (pesticides, pharmaceuticals). Two assumptions of this upscaling methodology (*i.e.,* involving equal adsorption capacities and surface diffusivities between the batch test and the fixed bed) were studied for the first time to investigate the aging effect on the adsorption capacity and kinetics of carbon at full scale. This study was conducted in natural waters (the Seine River) treated by Veolia Eau d'Ile de France in Choisy-Le-Roi, a division of Syndicat des Eaux d'Ile de France, aiming to monitor real industrial conditions. The isotherms showed that the adsorption capacity for most compounds was significantly affected by aging. For the mass transfer coefficients (*i.e.,* as determined by the homogeneous surface diffusion model (HSDM)), different patterns of adsorbate/adsorbent behaviors were observed, suggesting different competition mechanisms. The model predictions (*i.e.,* HSDM) performed with all parameters obtained during the batch tests tended to overestimate the full-scale pilot adsorption performance. This overestimation could be compensated for by applying a scaling factor. Finally, an empirical pseudo-first order function was used to model the impact of the GAC service time on the characteristic adsorption parameters. Thus, our scale-up procedure may enable the prediction of long-term fixed bed adsorption behaviors and increase the model efficiency for practical implementation.

1. Introduction

Adsorption on activated carbon is recognized as an efficient technology for emerging organic micropollutant (MP) removal in drinking water treatment plants (DWTPs) (Katsigiannis et al., 2015; Kennedy et al., 2015). The most common MP removal process is the application of a fixed bed reactor using granular activated carbon (GAC), where the carbon grains remain in place for several months or years. To optimize the industrial design and maintenance, numerical modeling is a useful tool to predict the MP removal efficiency. Among all the descriptive models, the homogeneous surface diffusion model (HSDM) is commonly used in number of studies to simulate adsorption processes at different scales (Bakir et al., 2014; Capelo-Neto and Buarque, 2016; Hand et al., 1997; Kim et al., 2016; Schideman et al., 2006a, 2006b; Zhang et al., 2009).

However, the estimation of HSDM parameters (*i.e.,* adsorption capacity and kinetics) in real industrial situations is complicated by the presence of natural organic matter (NOM) in waters not only due to its direct competition but also because of its preloading effect, mainly resulting in GAC aging. Number of previous researches have assessed the NOM preloading effect, showing a reduction in the adsorption capacities and kinetics with increasing NOM preloading time (Ding et al., 2006; Li et al., 2003; Schideman et al., 2006a, 2006b). Furthermore, these studies emphasized an accurate prediction of long-term fixed bed adsorption requisites by incorporating the NOM preloading effect into the modeling process.

Nevertheless, these studies have some limitations. First, all of studies used artificially in-lab preloaded GAC, which may not be representative of real full-scale GAC aging, especially regarding biofilm development. Second, some of the studies were conducted with a relatively high concentration of pollutants ($mg \cdot L^{-1}$), whereas the pollutant concentration in treated water (DWTP) ranges from $ng \cdot L^{-1}$ to $\mu g \cdot L^{-1}$. The adsorption behavior might be different for these

68 different concentrations. To date, few modeling studies have attempted to provide insight into

69 the effect of real fixed bed aging on pollutant adsorption at low concentrations for practical

70 industrial implementation.

71 Various methodologies can be used to estimate the two essential HSDM parameters. Pilot-

72 scale studies are the most accurate approach (Kennedy et al., 2015), but they are time-

73 consuming and expensive. To overcome their disadvantages, scale-down technologies such as

74 discontinuous tests (*i.e.,* perfectly mixed batch reactor (PMBR), differential column batch

75 reactor (DCBR)) and short-bed column tests (SBCTs) have been investigated (Hand et al.,

76 1984). Carter and Weber Jr. (1994) predicted the breakthrough curve of trichloroethylene in a

77 small-scale pilot using adsorption results in batch-scale studies. Their studies demonstrated

78 the feasibility of the upscaling method to predict fixed bed behavior; however, the studies are

79 restricted by high pollutant concentrations, the use of artificially preloaded GAC and a

80 relatively small-scale pilot verification.

81 Recent studies have attempted to simulate or predict full-scale pilot adsorption behavior with

82 pollutant concentrations of $ng \cdot L^{-1}$ or $\mu g \cdot L^{-1}$. Scharf et al. (2010) evaluated the adsorption

83 capacity with ground activated carbon particles in batch tests to simulate on-site pilot test data

84 over a two-year period. This approach is suitable for modeling but not for prediction. Later,

85 Capelo-Neto and Buarque (2016) applied all the adsorption parameters in batch studies to

86 predict the behavior of a hypothetical GAC filter, but the prediction results were not verified

87 by a full-scale pilot study. Regrettably, neither study considered the NOM preloading effect in

88 the modeling process, although the other experimental conditions approached the real DWTP

89 conditions.

90 Hence, our study was conducted under conditions that are representative of real DWTP

91 conditions by ensuring the same water quality as that used in real filters and ensuring a

4

92   pollutant concentration of ng·L^{-1} to µg·L^{-1}. In contrast to all previous studies using artificially

93   in-lab preloaded GACs, in this study, the GAC samples were collected through local coring

94   filters of various service times (from several months to years) at three different depths; thus,

95   these samples represent the actual GAC spatial and temporal aging process over most of its

96   service life.

97   The primary objective of this research is to develop and validate an upscaling methodology to

98   predict GAC fixed bed adsorption behaviors subject to the GAC aging effect. To achieve this

99   aim, the study is separated into three steps: (1) investigation of the GAC aging effect on the

100   adsorption capacity and kinetics using batch tests; (2) validation of the upscaling prediction

101   by full-scale industrial pilot tests; and (3) assessment of an empirical function of the aging

102   effect for practical implementation.

103

104   2. Materials and methods

105   2.1 Experimental methodology

106   The choice of scale-down approaches aims to guarantee an accurate determination of

107   adsorption parameters under controlled conditions. Adsorption isotherms were achieved using

108   ground and mixed GAC particles in PMBR according to Capelo-Neto and Buarque (2016)

109   and Scharf et al. (2010), with the assumption that the adsorption capacity determined by

110   mixing GACs from three depths can approximate the overall capacity of the fixed bed. Recent

111   works by Corwin and Summers (2010) and Kennedy et al. (2017) showed that the adsorption

112   kinetics of MPs (*i.e*., as for pesticides) with GAC was dominated by intraparticle diffusion

113   (pore diffusion and surface diffusion). The external mass transfer resistance was negligible in

114   both small-scale and pilot-scale column tests over the long term. Therefore, a differential

115 column batch reactor (DCBR) was employed here to determine the intraparticle diffusivity for

116 uncrushed aged GAC grains. This approach can minimize the external mass transfer influence

117 and enhance the accuracy of intraparticle diffusivity determination (Baup et al., 2000; Hand et

118 al., 1983).

119 Finally, an *in-situ* pilot-scale test was used to validate the proposed prediction methodology.

120 Uncrushed GACs from three depths were loaded in the same arrangement into pilot columns

121 to approximate the real spatial variation of local filters. The columns were fed with

122 deozonated water from the plant, spiked with a set of MPs.

123

2.2 Water quality

125 Pretreated surface water from the DWTP of Choisy-Le-Roi (France, supplying 1.8 million

126 people for the region of Ile de France) was used for all adsorption experiments. The influent

127 water for the pilot test was collected after the ozonation-deozonation step to maintain the

128 same water quality as that in the GAC filters in the DWTP. The water used for the batch tests

129 was collected at one time during the pilot test to minimize temporal fluctuations of influent

130 water. In addition, 30 mg·L^{-1} of sodium azide was added to the batch experiments to inhibit

131 biological activities. Carter and Weber Jr. (1994) showed that the addition of sodium azide

132 did not affect the adsorption process. Sodium azide was not added to the pilot tests to

133 represent real industrial conditions. Previous study (Kennedy et al., 2015) also emphasized

134 that the removal of MPs was governed by adsorption in similar conditions. Over the test

135 period (approximately 3 weeks), the water quality was almost stable, with an average total

136 organic carbon of approximately 2.3 mg·L^{-1} and a pH value close to 7.9.

137

6

138   **2.3 Target MPs**

139   Seventeen emerging organic MPs, including seven pharmaceutical compounds and ten

140   pesticides, were selected for this adsorption study in view of the MP occurrence in surface

141   and drinking water (Gasperi et al., 2009; Vulliet et al., 2011; Vulliet and Cren-Olivé, 2011)

142   and their removal efficiency by activated carbon (Bunmahotama et al., 2017, 2015; Mailler et

143   al., 2016). These MPs cover a wide range of physio-chemical properties, such as molar mass,

144   polarity and solubility to evaluate the robustness of our approach over a broad range of

145   properties for potential targets. The detailed information is provided in Supplementary

146   Material A (See **Table SA.1**). All compounds were of analytical purity and purchased from

147   Sigma-Aldrich (France).

148   The selected molecules were analyzed by ultra-high-pressure liquid chromatography (UHPLC)

149   coupled with tandem mass spectrometry (MS/MS) (Acquity, Waters, Quattro Premier,

150   Micromass, USA) following an online solid phase extraction (SPE) (Waters 2777). The

151   complete analytical procedure was previously described by Bazus et al. (2016) and was

152   adapted in this study to the target compounds by a slight modification of the elution gradient.

153   Briefly, separation was achieved within 13 minutes using an Acquity BEH C18 (2.1 x 100

154   mm – 1.7 μm) column and with a linear elution gradient achieved by increasing the

155   proportion of acetonitrile at a constant flow rate of 0.4 mL·min^{-1}. The chromatographic

156   conditions and multiple reaction monitoring (MRM) transitions are reported in **Table SA.2** in

157   Supplementary Material A.

158

159   **2.4 Activated carbon**

7

160 To investigate the influence of GAC aging on the adsorption capacities and kinetics, a virgin

161 GAC, namely, Aquasorb 1200 (Jacobi, France), was used as the reference for virgin GAC

162 filters, and three aged GACs were collected from local filters at three depths (0.5 m, 1 m and

163 2 m) from the DWTP of Choisy-Le-Roi, France. The GACs were in service for 6, 17.4 and 35

164 months with a treated bed volume of 20930, 56000 and 102000, respectively. The four GACs

165 were renamed C-0, C-6, C-17 and C-35, where the number represents the months of service of

166 the GAC.

167 For the batch tests, all GAC samples were first washed with pure water to remove fines and

168 dried at 60 °C to avoid destruction or modification of the NOM adsorbed on the GAC surface.

169 Then, for the equilibrium isotherm test, the same amount of GAC from the three depths was

170 mixed, crushed and sieved to obtain small-sized grains between 80 µm and 100 µm (the

171 specific areas of the GACs are shown in **Table SA.3**) to minimize the equilibrium time and

172 reduce the risk of degrading the target compounds. Patni et al. (2008) showed that crushed

173 GAC had the same specific area and micropore size volume fraction as the original GAC. For

174 batch kinetics tests, the fraction of 800/1000 µm was used by sieving the dried GAC grains of

175 each depth separately. However, the original GAC grains were used for pilot tests without any

176 pretreatment, and they were packed in accordance with the spatial arrangement of local filters

177 with the same amount of GAC from the three depths.

178

179 **2.5 Isotherm tests and kinetics batch tests**

180 Equilibrium adsorption capacities were evaluated using the bottle-point technique. A constant

181 mass of crushed GAC (2 mg·L^{-1}) was mixed using magnetic stirrers with MP concentrations

182 ranging from 1 to 10 µg·L^{-1} in 10 L of water at room temperature (25°C). The equilibrium

183 time was determined by following the adsorption kinetics in the middle concentration range,

184   and the kinetics evaluation showed that the adsorption reached equilibrium after 14 days.

185   Initial and residual concentrations of each compound were measured by SPE-UPLC-MS/MS

186   to determine the adsorption quantities according to **Eq. 1**:

187    $q_e = \frac{(C_0 - C_e) \cdot V_R}{m_{GAC}}$ (**Eq. 1**)

188   where q_e is the adsorbed quantity ($nmol \cdot g^{-1}$), C_0 and C_e are the initial and equilibrium solute

189   concentrations in the liquid phase, respectively ($nmol \cdot L^{-1}$), V_R is the reactor volume and m_{GAC}

190   is the quantity of GAC.

191   The kinetics studies were carried out in a DCBR with 100 mg of uncrushed GAC grains

192   (approximately 33.3 mg for each depth). The 10 L solution (1 $\mu g \cdot L^{-1}$ for each pollutant),

193   which was stored in a glass bottle equipped with a magnetic stirrer, was pumped with a

194   constant flow (peristaltic pump; 1.5 $L \cdot h^{-1}$) through a small plastic column (4.32 mm inner

195   diameter) containing the GAC grains, and then the solution was returned to the tank (**Fig.**

196   **SB.1** in Supplementary Material B).

197

2.6 Full-scale pilot design and experiments

199   The full-scale pilot was designed to be representative of the GAC filter units of the DWTP in

200   Choisy-Le-Roi, France (**Figure 1**). This pilot allows studying the breakthrough curves in 4

201   parallel 2 m columns simultaneously fed with the same water quality. Within the plant, the

202   water is withdrawn from the GAC feeding line into a mixing tank equipped with a back flow

203   preventer. Since the adsorbent at the bottom of the column requires approximately the same

204   amount of time for saturation as the GAC filters in the DWTP (typically many years),

205   determining the complete breakthrough curve is not reasonable. Therefore, the columns were

206   equipped with intermediate sampling points (every 25 cm) to determine the concentration-

207 depth profile at a given time or to determine the breakthrough curve at a given bed depth. The

208 columns consist of a 50 mm internal diameter cylinder (the height of the GAC filling is

209 approximately 1.2 m, which corresponds to an empty bed contact time of 7.2 minutes) of

210 polycarbonate. To avoid any entry of air bubbles into the GAC filter, the columns are topped

211 with a tank that is overflowing with water spiked with 1 µg·L^{-1} of each MP. An HPLC pump

212 is used to add 1.6 mL·min^{-1} of a 1 mg·L^{-1} stock solution into the main water flow. A flow rate

213 of 20 L·h^{-1} in each column was controlled at the outlet using a multichannel peristaltic pump.

214 The contact time and linear velocity (10 m·h^{-1}) corresponded to the common industrial

215 conditions of Veolia in Paris. Moreover, to ensure both a continuous operation and a reliable

216 comparison of the GAC performance between the pilot test and the real industrial fixed bed, a

217 2-hour backwash was applied for every 48-hour operation. Water samples were periodically

218 collected from each column at different bed depths through sampling ports and analyzed by

219 SPE-UPLC-MSMS.

220

221 **2.7 Model description**

222 Several modeling strategies have been proposed for the adsorption equilibrium of MPs in

223 water containing NOM. Studies (Bunmahotama et al., 2017; Smith et al., 1987; Zietzschmann

224 et al., 2014) have successfully shown the use of competition models that consider the NOM as

225 an "equivalent background compound". In the competition models, the optimized parameters

226 are obtained by fitting the model parameters to experimental data associated with a defined

227 error function. However, the application of the models is limited by common shortcomings.

228 These models require at least mixed isotherms in NOM-free and NOM-containing water to

229 obtain better fitting parameters. Furthermore, the fitting parameters are not transferable; hence,

230 for other water/GAC/MP system, complementary tests and fitting procedures are necessary to

231 re-determine these parameters.

232 Another model is a single 'apparent' component model, which has already been employed in

233 previous studies (Carter and Weber Jr., 1994; Scharf et al., 2010). In such a model, the

234 parameters are directly fitted to experimental data of the target compounds obtained in NOM-

235 containing water. Regarding the practical objective of our study, we limited ourselves to the

236 latter approach. The adsorption equilibrium of each target molecule was modeled by the

237 Freundlich model according to **Eq. 2**:

238 $$q_e = K \times C_e^{1/n} \tag{Eq. 2}$$

239 where q_e is calculated according to **Eq. 1**, K is Freundlich's coefficient (nmol·g^{-1}/[(nmol·L^{-1}

240 $^1)^{1/n}$], and n is Freundlich's exponent (dimensionless). The logarithmic transformation allows

241 the use of classical linear regression available in many spreadsheet software packages.

242 The HSDM was used to simulate batch kinetics and pilot breakthrough curves. The model

243 equations for DCBR and fixed bed are presented in **Table SA.4**, and these equations were

244 numerically solved using in-house software (Baup et al., 2000) that applied the orthogonal

245 collocation method to convert the partial differential equations into ordinary differential

246 equations with a function of approximation provided by Villadsen and Stewart (1967). The

247 resolution began with nondimensionalization of the equations to simplify the influence of

248 units. External mass transfer (characterized by the coefficient k_f) and surface diffusion

249 (characterized by the surface diffusion coefficient D_s) are the two potentially limiting steps for

250 adsorption kinetics. Their values can be determined by fitting experimental data. The

251 optimization solver's fitting criteria are the sum of least squares of the absolute difference

252 between the experimental and modeled concentrations at all sampling times. The Biot number

253 (**Eq. 3**) is introduced to interpret the predominant limiting step. When the Biot number > 100,

11

254   the whole kinetics process is controlled by surface diffusion; when the Biot number < 0.1, the

255   external mass transfer is predominant, and when the Biot number is between 0.1 and 100, the

256   adsorption kinetics is influenced by the two mechanisms. More details of the model

257   description can be found in many publications (Schideman et al., 2006a; Zhang et al., 2009).

258    $Biot = \frac{k_f \cdot R_p \cdot C_0}{D_s \cdot \rho_p \cdot q_0}$ (**Eq. 3**)

259   Here, R_p and ρ_p are the particulate radius and apparent density, respectively, and q_0 is the

260   adsorption capacity of carbon at concentration C_0.

261

3. Results and discussion

3.1 Effect of GAC aging on the adsorption capacity

264   The effect of GAC aging on the adsorption capacity was evaluated using isothermal

265   equilibrium tests with a virgin GAC (C-0) and three aged GACs (C-6, C-17 and C-35). The

266   obtained Freundlich model parameters (K and 1/n) can be found in **Table SA.5**. The

267   adsorption capacity of compounds (represented by q) is equal to the K value when the

268   concentration is fixed to 1 nmol·L^{-1}. To facilitate the comparison of the aging effect for

269   different compounds, the relative adsorption capacity was introduced. Instead of using the

270   virgin GAC as a reference, we used q/q_{max} since some compounds have a higher q value with

271   aged GAC than with virgin GAC.

272   **Figure 2** shows that the GAC aging effect on MP adsorption differs. Four behaviors can be

273   distinguished. For the pollutants of Group I, a continuous decrease in q is observed with

274   increasing aging time. The q values diminish sharply (approximate 50%) after the initial 6

275   months of use and continue to decrease at a similar or slightly slower rate with increasing age.

276 Compounds of Group II have a similar severe reduction in q values (more than 50%) at the

277 earlier aging stage. However, unlike Group I, the K values for these compounds remain stable

278 afterward (between 6 and 35 months of service). The two behaviors of Groups I and II have

279 been reported in previous studies (Carter and Weber Jr., 1994; Schideman et al., 2006a),

280 noting that the NOM accumulated successively at the GAC surface reduced adsorption

281 capacity due to pore blockage and pore competition.

282 For the compounds of Group III, a general reduction in q was observed for the three aged

283 GACs compared to the virgin GAC. However, after a strong initial decrease, the q values of

284 the three compounds increased with aging time. This irregular increase in adsorption capacity

285 is difficult to explain with the current competition mechanisms. Changes in the nature of the

286 biofilm might provide an explanation. Long-term studies of biofilm formation scare, but some

287 data indicate an evolution of the morphology and composition of the biofilm (Batté et al.,

288 2003; Gibert et al., 2013) during a long operation time, especially a reduction in the

289 carbohydrate content from a fresh biofilm to an older biofilm. Thus, these changes in the

290 biofilm nature might modify the affinity of GAC towards each molecule and contribute to the

291 biodegradation of molecules.

292 In Group IV, the experimental isotherm plots (**Fig. SB.2**) show no significant difference in

293 adsorption capacity between C-0 and C-6, whereas a serious reduction in adsorption capacity

294 is observed after long-term use. The behavior of the compounds in this group is generally

295 similar to the compounds of Group I but with a lag phase before the drop in the adsorption

296 capacity. A competition mechanism mentioned by Yu et al. (2009) can explain this lag phase.

297 At the initial preloading stage, the NOM with a low molecular weight diffuses rapidly into the

298 adsorption sites of the outer layers of the GAC, resulting in a serious reduction in the

299 adsorption potential of smaller molecules compared with larger molecules. As the molecules

300 of Group IV have the highest molecular weight, they were less impacted at this initial phase

13

301 but could be seriously affected when the NOM diffused simultaneously into the GAC inner

302 space during the later aging period.

303

304 **3.2 GAC aging influence on the adsorption kinetics**

305 The aging effect on the adsorption kinetics was first investigated by DCBR tests.

306 Experimental kinetics data obtained using the DCBR setup that was operated at initial

307 concentrations of 1 $\mu g \cdot L^{-1}$ in treated river water show no obvious difference from the aged

308 GACs (**Fig. SB.3**). However, the observed kinetics are influenced by both the adsorption

309 capacity and mass transfer. To separate these effects, the HSDM is applied using the

310 equilibrium data obtained in the previous section. The kinetics parameters are then determined

311 by fitting the external mass transfer coefficient (k_f) and internal surface diffusivity (D_s) to the

312 experimental data (the results are collected in **Table SA.6**).

313 The experimental plots can be satisfactorily fitted by HSDM for all pollutants, despite the

314 analytical uncertainties observed for some compounds at these low concentrations. Essentially,

315 the DCBR is designed to accurately estimate internal diffusion by minimizing or controlling

316 the influence of external diffusion. The parameter sensitivity for the model calibration is

317 interpreted by employing the Biot number. Relatively high Biot numbers (>50) are observed

318 for most molecules (**Table SA.6**), which suggests that the adsorption kinetics is indeed

319 mainly dominated by D_s. Thus, the following discussions focus only on the influence of GAC

320 aging on D_s. A relative surface diffusivity was introduced to simplify the presentation. The

321 D_s/D_{smax} ratio was also used since most compounds appear to have a higher D_s value with

322 aged GAC than with virgin GAC.

14

323 **Table SA.6** shows that the aging effect on D_s is complicated and might be differentiated into

324 two groups. As presented in **Figure 3**, Group I has the highest D_s value for virgin GAC; then,

325 this value greatly decreases at the earlier aging stage and stabilizes during the later aging

326 period, except for diuron, whose D_s values are not greatly impacted by the aging time. The

327 behavior of Group I was expected and has already been observed in previous studies (Carter

328 et al., 1992; Speth and Miltner, 1989). However, the behavior of Group II was observed for

329 the majority of molecules in which the D_s values reach the maximum after several months of

330 use followed by a decrease in the later stage. A hypothesis is presented to explain this

331 phenomenon. The adsorbed NOM, mainly in the macropores and mesopores, might change

332 the surface properties, thus reducing the affinity towards some compounds. Note that the

333 HSDM is based on the assumption that surface diffusion is largely predominant over porous

334 diffusion (Noll et al., 1991). A less attractive surface can increase the relative contribution of

335 porous diffusion, resulting in an apparent increase in the D_s value obtained using HSDM

336 fitting. Indeed, the measured diffusion coefficient is an apparent coefficient that represents the

337 two phenomena. Later in the process, the diffusion in the micropores will limit the mass

338 transfer process. These changes in the attractiveness of the surface might differentially affect

339 the various molecules and could explain the differences observed for the fitted D_s values.

340 The range of D_s covers several orders, making it difficult to highlight some internal

341 correlations. The logarithmic transformation ($pD_s = - Log_{10}(D_s)$) allows a better study of the

342 possible correlations among the GACs; the results are shown in **Table SA.7**. It appears that

343 the relationship of the pD_s values between the aged GACs and the virgin GAC is mostly

344 insignificant (the p values are relatively high), whereas a strong linear correlation of pD_s

345 values among aged GACs is observed (**Figure 4**). Thus, for practical implementation, it

346 seems that extrapolation of the experimental results carried out on virgin GAC to explain the

15

347 adsorption kinetics on aged GACs would lead to erroneous results, while the extrapolation

348 would be much more reliable with GAC that was already exposed to NOM.

349

3.3 Scale-up model development and validation

351 After investigating the aging effect on the adsorption capacity and kinetics in batch tests, a

352 scale-up procedure was carried out to predict the influence of aging on the fixed bed

353 adsorption behavior. The procedure assumes that the GAC in the fixed bed has the same

354 adsorption capacity and surface diffusivity as those during the batch experiment; therefore,

355 pilot breakthrough curves can be predicted by HSDM associated with these two parameters

356 determined in batch-scale studies. The external mass transfer coefficient is calculated by

357 empirical correlations from the literature because it is not scalable from batch-scale studies to

358 pilot-scale studies due to changes in flow in the reactor. The prediction results are finally

359 verified by full-scale pilot studies.

360 Only the breakthrough curves of atenolol at the upper two depths (approximately 12 and 37

361 cm) for 4 GACs are shown here (**Figure 5**) since the concentrations of samples taken at

362 deeper sampling points are below the quantification limits. The results obtained for all

363 molecules and GACs can be found in Supplemental Material B (**Fig. SB.4**). A 47% and 80%

364 removal efficiency of atenolol was achieved for 12 cm and 37 cm depths, respectively, with

365 virgin GAC after 250 hours of operation (**Figure 5 (a)**), corresponding to a throughput of

366 20833 and 6757 equivalent bed volumes (BVs), respectively. However, a slightly better

367 removal efficiency is observed for C-6 (**Figure 5 (b)**), which achieves 58% and more than 90%

368 removal at almost the same depths. Then, the removal efficiency decreased with aging time,

369 showing 54% and 88% for C-17 (**Figure 5 (c)**) and 41% and 72% for C-35 (**Figure 5 (d)**) at

370 the upper two depths, respectively.

16

371 The observed fixed bed behaviors of atenolol with the 4 GACs are consistent with the D_s

372 evolution in the batch kinetics tests; accordingly, the better removal performance of atenolol

373 with C-6 in the pilot tests is probably due to its faster mass transfer. The molecules penetrate

374 more rapidly into the pores of GAC, resulting in a lower molecular concentration in the outlet

375 flux (C/C_0). The good agreement between the GAC adsorption behaviors in the pilot test and

376 the D_s evolution in the batch test confirmed the feasibility of the proposed upscaling

377 prediction procedure if the pilot-scale studies are also controlled by surface diffusion.

378 Therefore, the prediction procedure was evaluated by estimating the external mass transfer

379 coefficient (k_f), which was initially estimated by several empirical correlations (Ohashi et al.,

380 1981; Ranz and Marshall Jr., 1952; Wakao and Funazkri, 1978; Wilson and Geankoplis, 1966)

381 (**Table SA.8**) and adjusted using, in particular, the first 20 hours of the breakthrough data. It

382 was intended to use empirical corrections for k_f; however, the model prediction with these

383 values underestimated the initial removal of compounds. The only adjustment of k_f improved

384 the predictions in the early stage, which also confirmed that the film diffusion controlled the

385 adsorption rate initially. The adjusted values (**Table SA.9**) are almost systematically 5-10

386 times greater than their estimations by the empirical correlations, possible because the

387 underlying assumption in the correlations is that particles are spherical, and no correction

388 factor is incorporated into the correlation formulas to compensate for the sphericity.

389 However, **Figure 5** shows that the predicted curves with equilibrium and surface diffusion

390 parameters obtained under batch conditions (represented by black continuous lines) are

391 generally located below the atenolol experimental data. This finding suggests an

392 overestimation of at least one of two "batch" parameters, either adsorption capacity or surface

393 diffusivity, or perhaps both. Several authors (Corwin and Summers, 2010; Kennedy et al.,

394 2017) have proposed introducing a scaling function of adsorption capacity or kinetics to

395 compensate for this overestimation for more accurate pilot modeling.

17

396   Accordingly, the first step was to determine an optimized modeling procedure for the pilot

397   results while keeping as many "batch" parameters as possible. It was decided to first adjust

398   the D_s value and to consider modifying the equilibrium parameters only in a second stage.

399   The reason for this choice is that the uncertainty of the surface diffusivity obtained through

400   the batch experiments is much larger than that of the isotherm parameters since the D_s value is

401   obtained using K and n. Another reason is that the breakthrough curves are only observed

402   over a relatively short period (nearly two weeks), while they are mostly kinetically driven. A

403   schematic description of the upscaling prediction procedure is shown in **Fig. SB.5**.

404   The prediction results with optimized D_s for atenolol are plotted in **Figure 5** (represented by

405   black discontinuous lines), showing a better agreement with the experimental data. The

406   adjusted D_s values and Biot numbers for all GACs can be found in **Table SA.9**. Similar to

407   batch kinetics, the Biot numbers for most molecules are relatively high, indicating that surface

408   diffusion controls the mass transfer processes for the pilot tests. This finding is in accordance

409   with a previous study (Kennedy et al., 2017).

410   Then, the correlation analysis considers only the fitted k_f values obtained when the Biot

411   number is below 100 because k_f values are not significant when the Biot number is greater

412   than 100; the results are reported in **Table SA.10** and **Figure 6 (a)**. Simultaneously, a

413   correlation analysis is also conducted with the pD_s values of the four GACs (see **Table SA.11**

414   and **Figure 6 (b)** for the results). The results show no significant correlations of k_f or D_s

415   between the virgin GAC and the aged GACs, but good correlations are observed among the

416   aged GACs. This result suggests that the extrapolation of k_f and D_s values for aged GACs is

417   reliable when using GAC that was already preloaded with the NOM rather than using the

418   virgin GAC.

419   Additionally, **Figure 7** shows that the behavior of surface diffusivity obtained by fitting fixed

420   bed experiments is very close to that observed from batch kinetics experiments (**Figure 3**);

421   their evolutions with GAC aging are similar, except for trimethoprim, ciprofloxacin and

422   propranolol. The cross correlations of pD_s between batch and fixed-bed tests are further

423   examined; however, no significant link between these tests was observed (**Figure 8**). **Figure 8**

424   shows that the range of variation of surface diffusion coefficients is approximately one to one

425   and a half orders of magnitude for the fixed bed, while it covers almost three orders of

426   magnitude for the batch values. Nevertheless, many points are close to the first bisector line,

427   indicating that for these compounds, the fixed bed D_s values can be easily obtained from the

428   batch data, whereas for other compounds, a scaling factor (SF) is required.

429   The investigation of the SF was then conducted for every compound and GAC, using the ratio

430   of the optimized pilot D_s value to the fitted DCBR D_s value. The results are summarized in

431   **Table SA.12**, which shows that the individual SF differs for compounds and GACs. However,

432   for several molecules, their individual SFs for the four GACs are very close, such as the SFs

433   for atenolol and atrazine, and especially for chlortoluron and diuron, whose individual SFs for

434   the four GACs are identical. Hence, a common SF for the four GACs was proposed by

435   minimizing the sum of the square error according to **Eq. 4**.

436     $$\sum error = \sum (\frac{D_{s\,pilot} - D_{s\,DCBR} * common\,SF}{D_{s\,pilot}})^2 \qquad \textbf{(Eq. 4)}$$

437   From **Table SA.12**, the 9 molecules (*i.e.*, atenolol, atrazine, chlortoluron, deisopropyl atrazine,

438   diuron, roxithromycin, propazine, tebuconazol) can be successfully scaled by a single

439   common SF ($\sum$Error < 1) (an example is shown in **Figure 9**), while a common SF cannot be

440   derived for other molecules.

441

3.4 Application of the time-variable empirical function

442

443 The above studies are mainly dedicated to finding upscaling approaches for fixed bed

444 prediction, while the relationships among the adsorption parameters and the aging time are

445 not well understood. Indeed, the adsorption isotherm and kinetics tests show that the evolution

446 of the adsorption capacity and rate with GAC aging time can be represented by a time-

447 variable empirical function (Carter and Weber Jr., 1994; Jarvie et al., 2005).

448 In the study by Carter and Weber Jr. (1994), they considered up to only 4 weeks of preloading;

449 hence, they proposed empirical functions having a generic form like **Eq. SA.1** (in the

450 Supplementary Material A) or a single linear relation with preloading time. Such a model is

451 not suitable here, as we have observed that most kinetics parameters exhibit a maximum value

452 during their time evolution.

453 Moreover, several studies demonstrated that the adsorption parameters were related to the

454 NOM surface loading rather than the preloading time since NOM preloading can be

455 significantly impacted by hydraulic conditions (especially the flow velocity) (Li et al., 2003)

456 and the NOM concentration. Corwin and Summers (2010) showed that mixing and repacking

457 of GAC media did not disrupt the mass transfer zone of the NOM, and the NOM surface

458 concentration of a given BV was identical. Therefore, the use of a BV for the time-variable

459 empirical function can successfully avoid the interference of the preloading time.

460 Hence, we propose a slightly different generic expression (**Eq. 5**) that can reproduce most of

461 the observed evolutions; an example of the fitted curves can be seen in **Figure 10**.

462 $$\frac{X(BV)}{X_0} = 1 - (a_X - b_X \cdot BV) \cdot \exp\left(-\frac{BV}{c_X}\right)$$ (**Eq. 5**)

463 where X is any adsorption parameter (K, n, k_f or D_s) for a given BV, X_0 is the value for virgin

464 activated carbon, and a_x, b_x and c_x are the empirical coefficients for parameter X. Nonlinear

20

465 regression analyses are carried out for all varying parameters with the defined function (**Eq.**

466 **5**), and the results are summarized in **Table SA.13 – SA.15**. All coefficients here are specific

467 to the given adsorbate/adsorbent/matrix experimental conditions and are not to be extended to

468 other cases, but the empirical functions give a relatively good prediction with low errors.

469 Therefore, the GAC aging effect on the adsorption capacity and kinetics in batch tests can be

470 assessed by the application of a time-variable empirical function for all target molecules.

471 However, this assessment is not enough for a pilot prediction since the breakthrough curves of

472 fixed bed tests cannot be directly simulated by batch parameters without an SF. Thus, for

473 further upscaling applications, the empirical function of D_s can be modified by the SF (**Eq. 6**):

474 $$\frac{D_s(BV)_{fixed-bed}}{D_{s0,batch}} = SF \cdot \left[1 - \left(a_{D_s} - b_{D_s} \cdot BV \right) \cdot \exp\left(-\frac{BV}{c_{D_s}} \right) \right]$$ (**Eq. 6**)

475 where the D_s value for the fixed bed prediction can be estimated at a given BV. Unfortunately,

476 while the values of the coefficients a_{D_s} and c_{D_s} from the DCBR data and the fixed bed data are

477 close for many compounds, this cannot be considered a generally acceptable assumption. A

478 smaller variation range of D_s values obtained from fixed bed data mainly affects the b_{D_s}

479 values.

480

4. Conclusions

482 The scale-up methodology based on the HSDM was tested as a feasible approach to predict

483 breakthrough curves of fixed beds with aged GAC. All the experiments, equilibrium, batch

484 kinetics and fixed bed dynamics were performed with real water that was withdrawn from a

485 drinking water treatment plant just before the GAC treatment unit and with the GAC sampled

486 from the plant's GAC filters to maximally maintain the real conditions. Several conclusions

487 can be drawn from this study:

488 • The adsorption capacities for MPs were well fitted by the Freundlich isotherm for both

489 virgin and aged GACs in the presence of NOM. A global reduction in the adsorption

490 capacity was observed for aged GACs compared to virgin GAC, which can be

491 explained by pore blockage and direct competition mechanisms. While an irregular

492 increase in the adsorption capacity was observed for three compounds with aged

493 GACs, this result suggested that biofilm evolution modified the surface interactions

494 towards these molecules.

495 • Adsorption kinetics in batch reactors and fixed bed reactors can successfully be

496 described by HSDM for all GACs. The adsorption kinetics for both experimental

497 scales was dominated by surface diffusion (D_s). Instead of a continuous reduction in

498 the D_s values with aging time, the D_s reached a maximum after several months of use

499 for more than half of the compounds in both reactor setups. A possible explanation for

500 this result was that modification of the surface properties by a biofilm contributed to

501 the porous diffusion, resulting in an apparent increase in the D_s value obtained using

502 HSDM fitting.

503 • The feasibility of the upscaling prediction procedure was evaluated via the adsorption

504 capacity and surface diffusivity obtained in batch-scale tests. This modeling approach

505 was finally verified by comparing the predicted breakthrough curves with the real

506 adsorption profiles in a real-scale fixed bed pilot test. The model prediction

507 overestimated the pilot adsorption performance for the majority of compounds when

508 the batch parameters were directly used. An SF for D_s could help to compensate for

509 the overestimation. However, its value appeared to be compound dependent. The

510 application of the above upscaling studies for fixed bed predictions, including the

511 direct use of batch parameters and the use of batch parameters with an SF, was

512   restricted to a portion of molecules because no clear global relationship was found

513   between the two scales used for the experimental tests.

514   • Finally, the aging effect on the adsorption capacities and kinetics was interpreted by a

515   new form of an empirical function that enabled reproducing the different forms of the

516   relative evolutions of equilibrium and kinetics parameters with aging time or bed

517   volume throughput. Although the empirical function is still an

518   adsorbent/adsorbate/matrix-dependent function, it provides insight into the aging

519   effect on the adsorption parameters. Combining this function with the SF, the

520   prediction for pilot adsorption behaviors is now possible. For industrial long-term

521   implementation, this scale-up prediction methodology associated with empirical

522   functions should facilitate the modeling approach.

523   This simulation approach remains interesting since all modeling parameters, such as

524   adsorption capacities and surface diffusion coefficients, determined in relatively short-term

525   economical batch tests could be used for fixed bed efficiency predictions. Although it is

526   beyond the scope of this study, qualitative and quantitative structure-activity relationships

527   should be considered to interpret the influence of the nature of the compounds, the GACs or

528   the water quality on the SF or coefficients of the time-variable empirical functions. This

529   methodology might offer a useful simulation approach for industrial design.

530

531

535 for the financial support. We also appreciate the cooperation of VEDIF and SEDIF for

536 making this study possible at the drinking water treatment plant of Choisy-Le-Roi.

537

538

539 **Reference**

540 Bakir, A., Rowland, S.J., Thompson, R.C., 2014. Transport of persistent organic pollutants by

541   microplastics in estuarine conditions. Estuar. Coast. Shelf Sci. 140, 14–21.

542   https://doi.org/10.1016/j.ecss.2014.01.004

543 Batté, M., Koudjonou, B., Laurent, P., Mathieu, L., Coallier, J., Prévost, M., 2003. Biofilm

544   responses to ageing and to a high phosphate load in a bench-scale drinking water system.

545   Water Res. 37, 1351–1361. https://doi.org/10.1016/S0043-1354(02)00476-1

546 Baup, S., Jaffre, C., Wolbert, D., Laplanche, A., 2000. Adsorption of pesticides onto granular

547   activated carbon: Determination of surface diffusivities using simple batch experiments.

548   Adsorption 6, 219–228. https://doi.org/10.1023/A:1008937210953

549 Bazus, L., Cimetiere, N., Wolbert, D., Randon, G., 2016. Development of on-line solid-phase

550   extraction-liquid chromatography coupled with tandem mass spectrometry method to

551   quantify pharmaceutical, glucuronide conjugates and metabolites in water. J. Chromatogr.

552   Sep. Tech. 7, 1–10. https://doi.org/10.4172/2157-7064.1000337

553 Bunmahotama, W., Hung, W.-N., Lin, T.-F., 2017. Prediction of the adsorption capacities for

554   four typical organic pollutants on activated carbons in natural waters. Water Res. 111,

555   28–40. https://doi.org/10.1016/j.watres.2016.12.033

556 Bunmahotama, W., Hung, W., Lin, T.-F., 2015. Predicting the adsorption of organic

557   pollutants from water onto activated carbons based on the pore size distribution and

558   molecular connectivity index. Water Res. 85, 521–531.

559   https://doi.org/10.1016/j.watres.2015.08.008

560   Capelo-Neto, J., Buarque, N.M.S., 2016. Simulation of saxitoxins adsorption in full-scale

561   GAC filter using HSDM. Water Res. 88, 558–565.

562   https://doi.org/10.1016/j.watres.2015.10.048

563   Carter, M.C., Weber Jr., W.J., 1994. Modeling adsorption of TCE by activated carbon

564   preloaded by background organic matter. Environ. Sci. Technol. 28, 614–623.

565   https://doi.org/10.1021/es00053a013

566   Carter, M.C., Weber Jr, W.J., Olmstead, K.P., 1992. Effects of background dissolved organic

567   matter on TCE adsorption by GAC. J. Am. Work. Assoc. 84, 81–91.

568   https://doi.org/10.1002/j.1551-8833.1992.tb07415.x

569   Corwin, C.J., Summers, R.S., 2010. Scaling trace organic contaminant adsorption capacity by

570   granular activated carbon. Environ. Sci. Technol. 44, 5403–5408.

571   https://doi.org/10.1021/es9037462

572   Ding, L., Mariñas, B.J., Schideman, L.C., Snoeyink, V.L., Li, Q., 2006. Competitive effects

573   of natural organic matter: Parametrization and verification of the three-component

574   adsorption model COMPSORB. Environ. Sci. Technol. 40, 350–356.

575   https://doi.org/10.1021/es050409u

576   Gasperi, J., Garnaud, S., Rocher, V., Moilleron, R., 2009. Priority pollutants in surface waters

577   and settleable particles within a densely urbanised area: Case study of Paris (France). Sci.

578   Total Environ. 407, 2900–2908. https://doi.org/10.1016/j.scitotenv.2009.01.024

579   Gibert, O., Lefèvre, B., Fernández, M., Bernat, X., Paraira, M., Pons, M., 2013. Fractionation

580   and removal of dissolved organic carbon in a full-scale granular activated carbon filter

581   used for drinking water production. Water Res. 47, 2821–2829.

582   https://doi.org/10.1016/j.watres.2013.02.028

583   Hand, D.W., Crittenden, J.C., Hokanson, D.R., Bulloch, J.L., 1997. Predicting the

584   performance of fixed-bed granular activated carbon adsorbers. Water Sci. Technol. 35,

585   235–241. https://doi.org/10.1016/S0273-1223(97)00136-4

586   Hand, D.W., Crittenden, J.C., Thacker, W.E., 1984. Simplified models for design of fixed-bed

587   adsorption systerms. J. Environ. Eng. 110, 440–456.

588   https://doi.org/10.1061/(ASCE)0733-9372(1984)110:2(440)

589   Hand, D.W., Crittenden, J.C., Thacker, W.E., 1983. User-oriented batch reactor solutions to

590   the homogeneous surface diffusion model. J. Environ. Eng. 109, 82–101.

591   https://doi.org/10.1061/(ASCE)0733-9372(1983)109:1(82)

592   Jarvie, M.E., Hand, D.W., Bhuvendralingam, S., Crittenden, J.C., Hokanson, D.R., 2005.

593   Simulating the performance of fixed-bed granular activated carbon adsorbers: Removal

594   of synthetic organic chemicals in the presence of background organic matter. Water Res.

595   39, 2407–2421. https://doi.org/10.1016/j.watres.2005.04.023

596   Katsigiannis, A., Noutsopoulos, C., Mantziaras, J., Gioldasi, M., 2015. Removal of emerging

597   pollutants through granular activated carbon. Chem. Eng. J. 280, 49–57.

598   https://doi.org/10.1016/j.cej.2015.05.109

599   Kennedy, A.M., Reinert, A.M., Knappe, D.R.U., Ferrer, I., Summers, R.S., 2015. Full- and

600   pilot-scale GAC adsorption of organic micropollutants. Water Res. 68, 238–248.

601   https://doi.org/10.1016/j.watres.2014.10.010

602   Kennedy, A.M., Reinert, A.M., Knappe, D.R.U., Summers, R.S., 2017. Prediction of full-

603   scale GAC adsorption of organic micropollutants. Environ. Eng. Sci. 34, 496–507.

604   https://doi.org/10.1089/ees.2016.0525

605   Kim, Y., Bae, J., Park, H., Suh, J.-K., You, Y.-W., Choi, H., 2016. Adsorption dynamics of

606   methyl violet onto granulated mesoporous carbon: Facile synthesis and adsorption

607   kinetics. Water Res. 101, 187–194. https://doi.org/10.1016/j.watres.2016.04.077

608   Li, Q., Mariñas, B.J., Snoeyink, V.L., Campos, C., 2003. Three-component competitive

609   adsorption model for flow-through PAC systems. 1. Model development and verification

610   with a PAC/membrane system. Environ. Sci. Technol. 37, 2997–3004.

611   https://doi.org/10.1021/es020989k

612   Mailler, R., Gasperi, J., Coquet, Y., Derome, C., Buleté, A., Vulliet, E., Bressy, A., Varrault,

613   G., Chebbo, G., Rocher, V., 2016. Removal of emerging micropollutants from

614   wastewater by activated carbon adsorption: Experimental study of different activated

615   carbons and factors influencing the adsorption of micropollutants in wastewater. J.

616   Environ. Chem. Eng. 4, 1102–1109. https://doi.org/10.1016/j.jece.2016.01.018

617   Noll, K.E., Gounaris, V., Hou, W.-S., 1991. Adsorption technology for air and water pollution

618   control. LEWIS PUBLISHERS, INC., Michigan, USA.

619   Ohashi, H., Sugawara, T., Kikuchi, K., Konno, H., 1981. Correlation of liquid-side mass

620   transfer coefficient for single particle and fixed-beds. J. Chem. Eng. Japan 14, 433–438.

621   https://doi.org/10.1252/jcej.14.433

622   Patni, A.G., Ludlow, D.K., Adams, C.D., 2008. Characteristics of ground granular activated

623   carbon for rapid small-scale column tests. J. Environ. Eng. 134, 216–221.

624   https://doi.org/10.1061/(ASCE)0733-9372(2008)134:3(216)

625   Ranz, W.E., Marshall Jr., W.R., 1952. Evaporation from drops - Part 1. Chem. Eng. Prog. 48,

626   141–148. https://doi.org/10.1016/S0924-7963(01)00032-X

627   Scharf, R.G., Johnston, R.W., Semmens, M.J., Hozalski, R.M., 2010. Comparison of batch

628   sorption tests , pilot studies , and modeling for estimating GAC bed life. Water Res. 44,

629   769–780. https://doi.org/10.1016/j.watres.2009.10.018

630   Schideman, L.C., Mariñas, B.J., Snoeyink, V.L., Campos, C., 2006a. Three-component

631   competitive adsorption model for fixed-bed and moving-bed granular activated carbon

632   adsorbers. Part I. Model development. Environ. Sci. Technol. 40, 6805–6811.

633   https://doi.org/10.1021/es060603w

634   Schideman, L.C., Mariñas, B.J., Snoeyink, V.L., Campos, C., 2006b. Three-component

635   competitive adsorption model for fixed-bed and moving-bed granular activated carbon

636   adsorbers. Part II. Model parameterization and verification. Environ. Sci. Technol. 40,

637   6812–6817. https://doi.org/10.1021/es060603w

638   Smith, E.H., Tseng, S., Weber Jr., W.J., 1987. Modeling the adsorption of target compounds

639   by GAC in the presence of background dissolved organic matter. Environ. Prog. 6, 18–

640   25. https://doi.org/10.1002/ep.670060119

641   Speth, T.F., Miltner, R.J., 1989. Effect of preloading on the scale-up of GAC microcolumns. J.

642   Am. Water Work. Assoc. 81, 141–148.

643   Villadsen, J. V., Stewart, W.E., 1967. Solution of Boundary Value Problems by Orthogonal

644   collocation. Chem. Eng. Sci. 22, 1483–1501. https://doi.org/10.1016/0009-

645   2509(96)81831-8

646   Vulliet, E., Cren-Olivé, C., 2011. Screening of pharmaceuticals and hormones at the regional

647   scale, in surface and groundwaters intended to human consumption. Environ. Pollut. 159,

648   2929–2934. https://doi.org/10.1016/j.envpol.2011.04.033

649 Vulliet, E., Cren-Olivé, C., Grenier-Loustalot, M.-F., 2011. Occurrence of pharmaceuticals

650 and hormones in drinking water treated from surface waters. Environ. Chem. Lett. 9,

651 103–114. https://doi.org/10.1007/s10311-009-0253-7

652 Wakao, N., Funazkri, T., 1978. Effect of fluid dispersion coefficients on particle-to-fluid mass

653 transfer coefficients in packed beds. Chem. Eng. Sci. 33, 1375–1384.

654 https://doi.org/10.1016/0009-2509(78)85120-3

655 Wilson, E.J., Geankoplis, C.J., 1966. Liquid mass transfer at very low reynolds numbers in

656 packed beds. Ind. Eng. Chem. Fundam. 5, 9–14. https://doi.org/10.1021/i160017a002

657 Yu, Z., Peldszus, S., Huck, P.M., 2009. Adsorption of selected pharmaceuticals and an

658 endocrine disrupting compound by granular activated carbon. 1. Adsorption capacity and

659 kinetics. Environ. Sci. Technol. 43, 1467–1473. https://doi.org/10.1021/es801961y

660 Zhang, Q., Crittenden, J., Hristovski, K., Hand, D., Westerhoff, P., 2009. User-oriented batch

661 reactor solutions to the homogeneous surface diffusion model for different activated

662 carbon dosages. Water Res. 43, 1859–1866. https://doi.org/10.1016/j.watres.2009.01.028

663 Zietzschmann, F., Worch, E., Altmann, J., Ruhl, A.S., Sperlich, A., Meinel, F., Jekel, M.,

664 2014. Impact of EfOM size on competition in activated carbon adsorption of organic

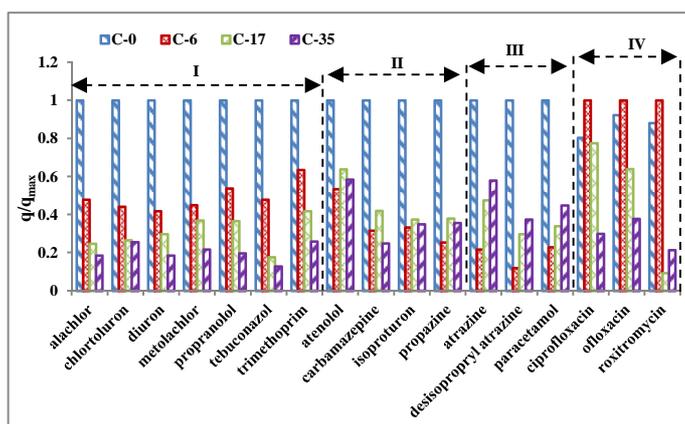665 micro-pollutants from treated wastewater. Water Res. 65, 297–306.

666 https://doi.org/10.1016/j.watres.2014.07.043

667
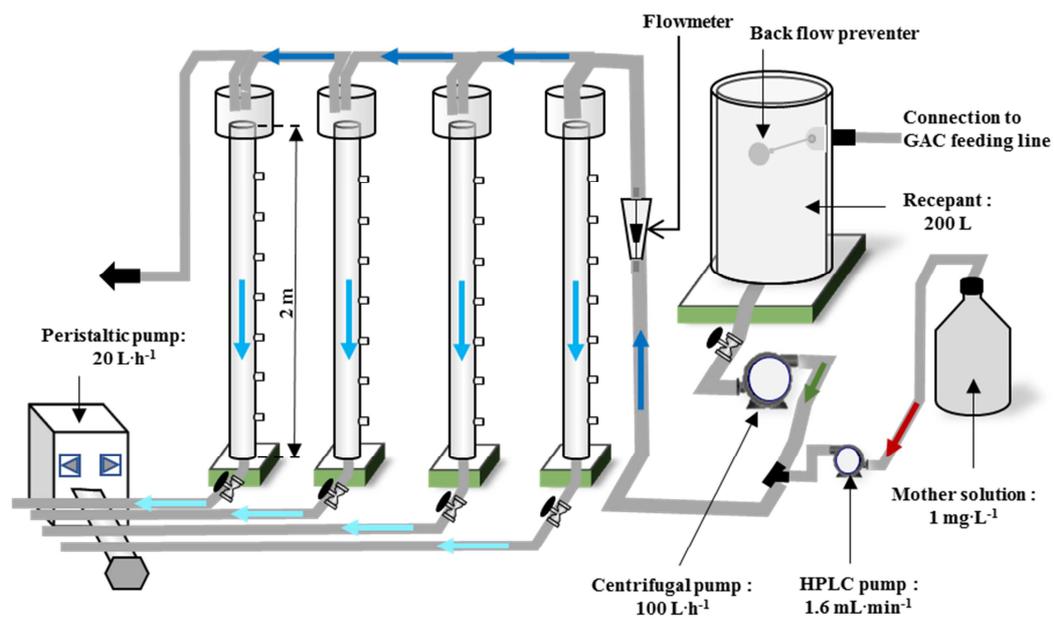
Figure 1: Schematic description of the full-scale pilot installation
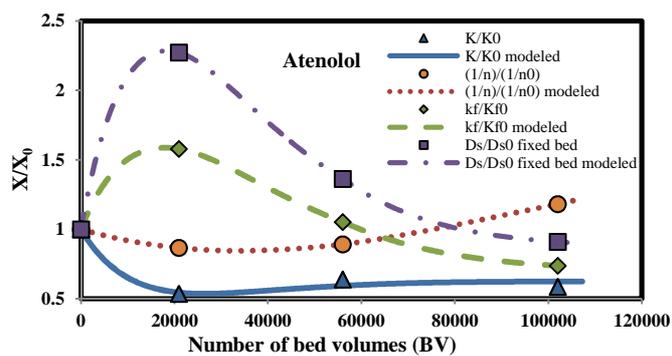
Figure 10: Example of fitted timely correlations for the various equilibrium and kinetic parameters of fixed bed HDSM model compared to the experimental data.

Figure 2: Relative adsorption capacities of micropollutants (q value compared to maximum q value of the four GACs) with various aged GACs (C-0, C-6, C-17 and C-35 represent respectively the virgin GAC and the aged GACs being in service for 6, 17 and 35 months). Four different groups of behaviors, labeled I to IV, are identified.
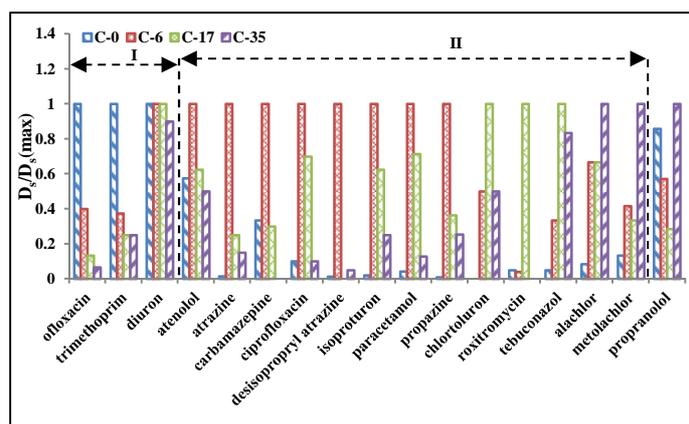
Figure 3: Relative surface diffusivities of micropollutants (D_s value compared to maximum D_s value of the four GACs) with various aged GACs (C-0, C-6, C-17 and C-35 represent respectively the virgin GAC and the aged GACs being in service for 6, 17 and 35 months). Two different groups of behaviors with exception of propranolol, labeled I to II, are identified.
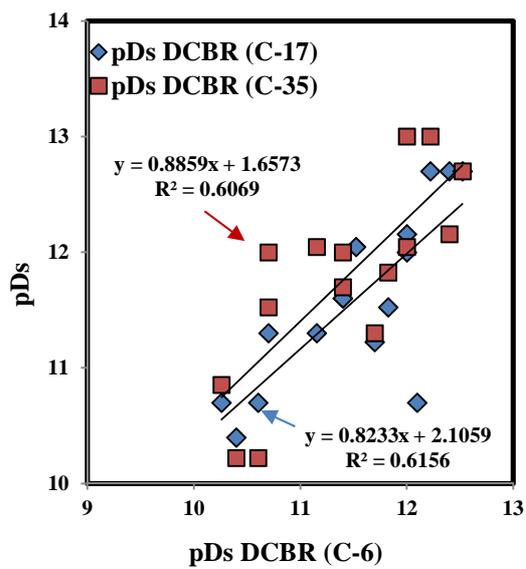
**Figure 4**: Correlation analysis of the pD_s values for DCBR setup among the aged GACs
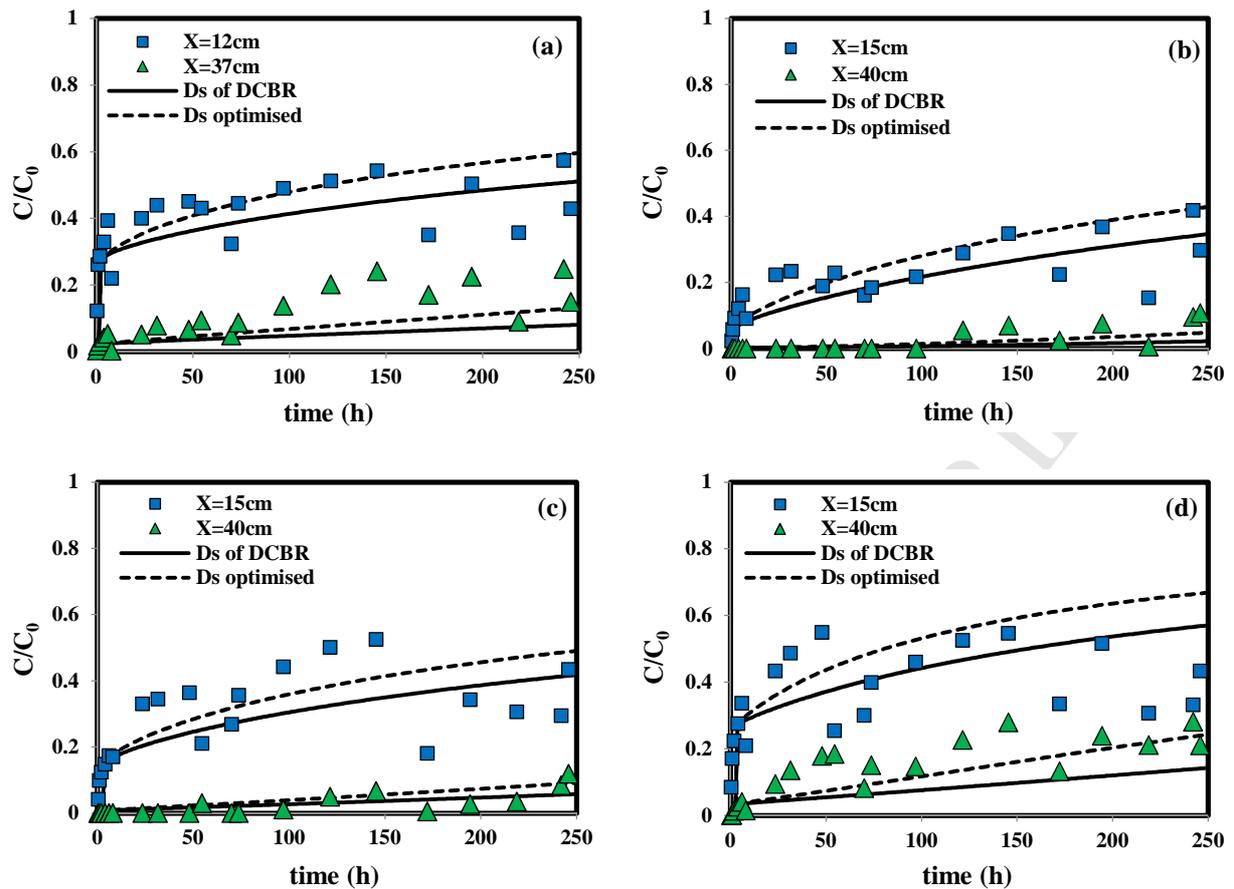
Figure 5: Breakthrough curves of atenolol with 4 GACs at the two depths: (a) C-0; (b) C-6; (c) C-17 and (d) C-35. Continued black line is HSDM modeling curve with D_s value obtained in DCBR setup, discontinued black line is HSDM modeling curve with optimized D_s value.
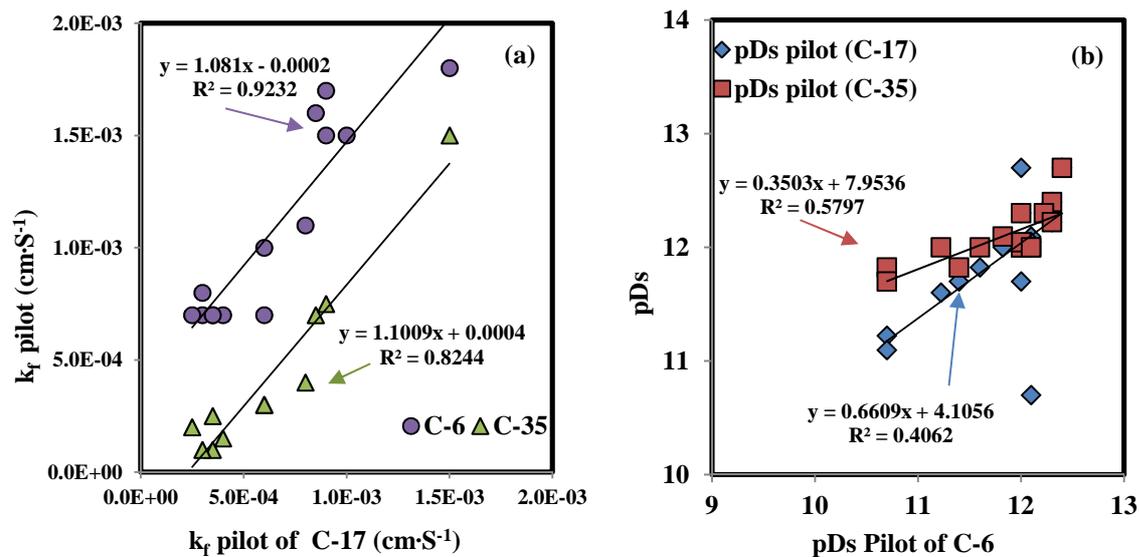
Figure 6: (a) Correlation among the fitted k_f values for full-scale pilot of virgin and aged GAC for the various compounds (k_f values have been discarded when the Biot number exceeded 100); (b) Correlation analysis of the pD_s values for full-scale pilot of aged GACs
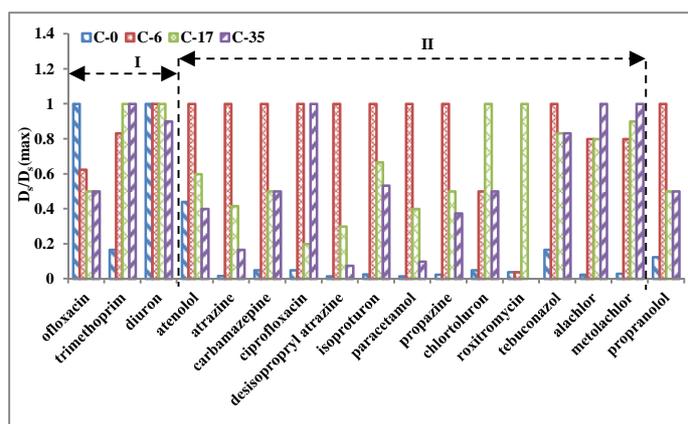
Figure 7: Time evolution of relative D_s values obtained from the fixed bed experiments. Group I and II are those defined in **Figure 3**.
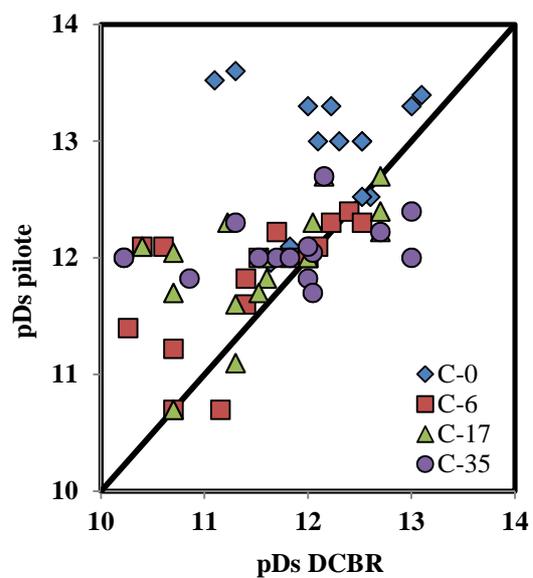
Figure 8: Cross correlation of pD_s values between the fixed bed and the batch kinetics tests of the 4 different GACs
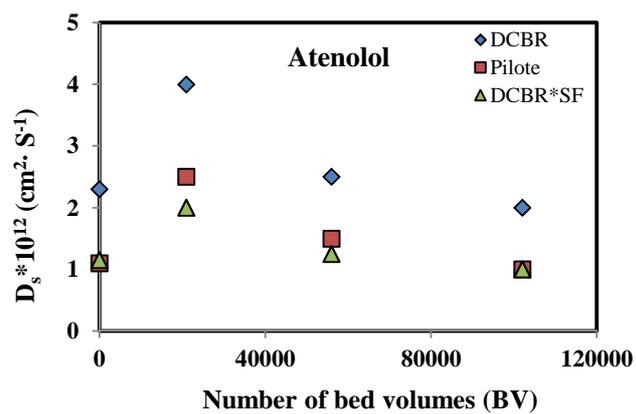
Figure 9: Example of application of scaling factor (SF)

Highlights:

- Adsorption capacities of the GAC reduced seriously after the 6 months of use

- D_s reached maximum after several months of use followed by a decrease

- An SF was required to predict the adsorption behaviors of the fixed bed

- A new pseudo-first order function was employed to model the impact of GAC

  aging on the adsorption parameters